Deficient Tryptophan Catabolism along the Kynurenine Pathway Reveals That the Epididymis Is in a Unique Tolerogenic State

Aicha Jrad-Lamine, Joëlle Henry-Berger, Pascal Gourbeyre, Christelle Damon-Soubeyrand, Alain Lenoir, Lydie Combaret, Fabrice Saez, Ayhan Kocer, Shigenobu Tone, Dietmar Fuchs, et al.

THE JOURNAL OF BIOLOGICAL CHEMISTRY VOL. 286, NO. 10, pp. 8030–8042, March 11, 2011

Deficient Tryptophan Catabolism along the Kynurenine Pathway Reveals That the Epididymis Is in a Unique Tolerogenic State*

Received for publication, August 4, 2010, and in revised form, November 23, 2010 Published, JBC Papers in Press, December 28, 2010, DOI 10.1074/jbc.M110.172114

Aicha Jrad-Lamine,[a1] Joelle Henry-Berger,[a] Pascal Gourbeyre,[b] Christelle Damon-Soubeyrand,[a] Alain Lenoir,[a] Lydie Combaret,[c] Fabrice Saez,[a] Ayhan Kocer,[a] Shigenobu Tone,[d] Dietmar Fuchs,[e] Wentao Zhu,[f] Peter J. Oefner,[f] David H. Munn,[g,h] Andrew L. Mellor,[g,i] Najoua Gharbi,[j] Rémi Cadet,[a] R. John Aitken,[k] and Joël R. Drevet[a2]

From the [a]GReD, CNRS UMR 6247/INSERM U931, Clermont Université, 24 Avenue des Landais, BP 80026, 63171 Aubière Cedex, France, [b]Institut National de Le Recherche Agronomique-Biopolymères, Interactions, Assemblages, 44316 Nantes Cedex, France, [c]Institut National de Le Recherche Agronomique, UMR 1019, UNH, CRNH Auvergne and Clermont Université, Unité de Nutrition Humaine, BP10448, F-63000 Clermont-Ferrand, France, the [d]Department of Biochemistry, Kawasaki Medical School, Okayama 701-0192, Japan, the [e]Division of Biological Chemistry, Biocentre, Innsbruck Medical University, 6020 Innsbruck, Austria, the [f]Institute of Functional Genomics, University of Regensburg, 93053 Regensburg, Germany, the [g]Immunotherapy Center and Departments of [h]Pediatrics and [i]Medicine, Medical College of Georgia, Augusta, Georgia 30912, the [j]Faculté des Sciences de Tunis, Département de Biologie, Université de Tunis El Manar, Mutuelleville, 1060 Tunis, Tunesia, and the [k]Australian Research Council Centre of Excellence in Biotechnology and Development, School of Environmental and Life Sciences, University of Newcastle, Callaghan, NSW 2308, Australia

Indoleamine 2,3-dioxygenase (IDO) is the first and rate-limiting enzyme of tryptophan catabolism through the kynurenine pathway. Intriguingly, IDO is constitutively and highly expressed in the mammalian epididymis in contrast to most other tissues where IDO is induced by proinflammatory cytokines, such as interferons. To gain insight into the role of IDO in the physiology of the mammalian epididymis, we studied both wild type and *Ido1*$^{-/-}$-deficient mice. In the caput epididymis of *Ido1*$^{-/-}$ animals, the lack of IDO activity was not compensated by other tryptophan-catabolizing enzymes and led to the loss of kynurenine production. The absence of IDO generated an inflammatory state in the caput epididymis as revealed by an increased accumulation of various inflammation markers. The absence of IDO also increased the tryptophan content of the caput epididymis and generated a parallel increase in caput epididymal protein content as a consequence of deficient proteasomal activity. Surprisingly, the lack of IDO expression had no noticeable impact on overall male fertility but did induce highly significant increases in both the number and the percentage of abnormal spermatozoa. These changes coincided with a significant decrease in white blood cell count in epididymal fluid compared with wild type mice. These data provide support for IDO playing a hitherto unsuspected role in sperm quality control in the epididymis involving the ubiquitination of defective spermatozoa and their subsequent removal.

Indoleamine 2,3-dioxygenase (IDO)[3] (EC 1.13.11.42) is the first and rate-limiting enzyme in Trp catabolism through the kynurenine pathway (Fig. 1). IDO is a ubiquitously expressed cytoplasmic protein typically activated by interferons (IFNs) (1–5). There is ample evidence that IDO mediates potent immunosuppression in classical immune responses as well as in fetal tolerance, tumor immune resistance, and regulation of autoimmune responses (1–3, 6–8).

Thirty years ago, Yoshida *et al.* (9) reported that rodent epididymal protein extracts exhibited a high IDO activity. Later, Takikawa *et al.* (10) demonstrated that unlike the classical cytokine-mediated expression of IDO encountered in nearly all mammalian tissues, the epididymal expression of IDO was constitutive and independent of IFN-γ. More recently, we have shown that IDO is expressed in a regionalized manner by both the principal and the apical cells of the most proximal epididymal region, the caput epididymis. To gain insights into the functions of IDO and the intermediates of the kynurenine pathway in the physiology of the mammalian epididymis, we measured the expression of IDO and related enzymes as well as the abundance of kynurenines and other Trp metabolites in both wild type (WT) and *Ido1*$^{-/-}$ male mice. These data were correlated with light and electron microscopic analyses of epididymal epithelium, sperm count, sperm morphology, and fertility.

EXPERIMENTAL PROCEDURES

Animals—The present study was approved by the Regional Ethics Committee in Animal Experimentation (Authorization CE2-04) and adhered to the current legislation on animal experimentation in France. Wild type and *Ido*$^{-/-}$ BALB/c male mice (11) aged 6 months were used throughout the study unless otherwise indicated. Mice were housed under controlled environmental conditions (temperature 22 °C, 12-h dark period), fed a basal diet (Global diet, 2016S, Harlan, Gannat, France) *ad libitum*, and given free access to water. For fertility testing, vir-

* This work was supported by grants from the French Ministry of Higher Education, CNRS, and INSERM (to J. R. D.). This work was also supported by grants from BayGene (to P. J. O.) and the Australian Research Council (to R. J. A.).

[1] Supported by a fellowship from the French Society of Andrology.

[2] To whom correspondence should be addressed. Tel.: 33-4-73-40-74-13; Fax: 33-4-73-40-52-45; E-mail: joel.drevet@univ-bpclermont.fr.

[3] The abbreviations used are: IDO, indoleamine 2,3-dioxygenase; TDO, tryptophan 2,3-dioxygenase; DPN, days postnatal; ESI, electrospray ionization; KYN, kynurenine; KA, kynurenic acid; AMC, 7-amido-4-methylcoumarin; Ub, ubiquitin; HK, 3-hydroxykynurenine; INDOL, indoleamine 2,3-dioxygenase-like; bNa, β-naphthylamide.

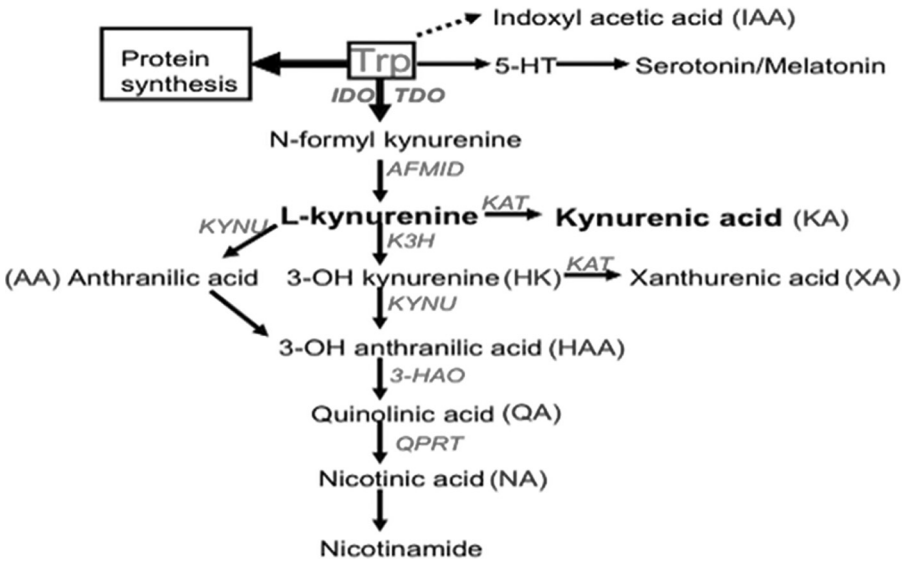

FIGURE 1. **Scheme of mammalian tryptophan catabolism.** Briefly, in mammalian cells, tryptophan is used mostly for protein synthesis. In a second quantitatively important pathway (driven by IDO in most cell types and by TDO more specifically in liver cells), it is the starting point of the kynurenine pathway. The kynurenine pathway gives birth to several metabolites, providing the appropriate enzymes that metabolize the various kynurenine intermediates are expressed. The main route of the kynurenine pathway leads to the formation of *N*-formyl kynurenine, L-kynurenine, 3-hydroxykynurenine, 3-hydroxyanthranilic acid, quinolinic acid, nicotinic acid, and *in fine* nicotinamine adenine dinucleotides. Additional lateral branches of the kynurenine pathway lead to the formation of other terminal kynurenines, such as KA, xanthurenic acid, and anthranilic acid. Kynurenines indicated in *boldface type* (*i.e.* L-kynurenine and KA) correspond to the most abundant kynurenines found in caput epididymal tissue. Outside the kynurenine pathway, tryptophan is also the precursor of serotonin and melatonin. A very small proportion of tryptophan is also transformed into indol derivatives, such as indoxyl acetic acid. Conversion of Trp to *N*-formyl kynurenine is achieved via IDO and/or TDO. Kynurenine intermediates and terminal kynurenines are produced through the action of several distinct enzymes, including formaminase (arylformamidase; *AFMID*), kynurenine aminotransferase (*KAT*; also known as AADAT), kynureninase (*KYNU*), kynurenine 3-hydroxylase (*K3H*; also known as KMO), and 3-hydroxyamino oxidase (*3HAO*).

gin 10-week-old BALB/c females were used. Wild type and *Ido*$^{-/-}$ male mice were killed by decapitation.

Immunohistochemistry—After deparaffinization and rehydration, endogenous peroxidases were inhibited with 0.3% (v/v) aqueous H_2O_2 (Sigma-Aldrich) for 30 min at ambient temperature, followed by blocking of the sections in PBS/bovine serum albumin (BSA) (1% (w/v); Euromedex, Mundosheim, France) for 30 min. In-house rabbit polyclonal anti-IDO (1:1000) (11) was incubated overnight at 4 °C. Sections were washed for 5 min in PBS and incubated for 1 h with biotin-SP-conjugated AffiniPure goat anti-rabbit IgG (H + L) antibody (1:500 in PBS/BSA 0.1%, Jackson ImmunoResearch Laboratories, Inc. (West Grove, PA)). After a wash in PBS, sections were incubated for 30 min with peroxidase-conjugated streptavidin (1:500 in PBS; Jackson ImmunoResearch Laboratories) and developed with the Vector NovaRED substrate kit for peroxidase (Vector Laboratories, Burlingame, CA).

RT-PCR and Semiquantitative Analysis—RT-PCR was used to amplify the transcripts of IDO, tryptophan 2,3-dioxygenase (TDO; EC 1.13.11.11), INDOL1 (indoleamine 2,3-dioxygenase-like 1, EC 1.13.11.52), arylformamidase (EC 3.5.1.9), kynureninase (EC 3.7.1.3), kynurenine aminotransferase (EC 2.6.1.7), and kynurenine 3-hydroxylase (EC 1.14.13.9) in mouse epididymal total RNA extracts. One μg of total RNA was reverse transcribed using ImPromII reverse transcriptase according to the manufacturer's instructions (Promega Corp., Madison, WI). For each sequence, specific primers were used (see Table 1). Amplification of GAPDH served as a semiquantitative control. Relative transcript levels of Trp-catabolizing enzymes in mouse caput epididymal RNA extracts of WT and *Ido*$^{-/-}$ animals were compared with those in lung tissue of the same animals. PCR amplifications were carried out as described earlier (12) with 2 μl of reverse-transcribed mixture using 1 unit of *Taq* polymerase (New England Biolabs) on different tissue samples (minimum $n = 3$). Suppression of spermatogenesis was achieved via busulfan (1,4-butanediol dimethanesulfonate) treatment (Sigma-Aldrich). Busulfan (35 mg/kg) diluted in dimethyl sulfoxide (50%) was inoculated intraperitoneally in animals (two injections at 15 and 22 days postnatal (DPN). Animals were then sacrificed at 30 DPN.

Western Blots—Proteins (40 μg) were separated by SDS-PAGE and transferred onto nitrocellulose membrane (Hybond ECL, GE Healthcare Biosciences). Blots were blocked with 10% low fat dried milk, 0.1% Tween 20, Tris base salt (TBS) and probed overnight at 4 °C with anti-GAPDH (1:5000, Sigma-Aldrich), anti-mTor, anti-phosphorylated mTor, anti-p70S6K, anti-phosphorylated p70S6K, and anti-beclin-1/ATG6. Secondary antibody was a goat anti-rabbit horseradish peroxidase conjugate (1:5000; GE Healthcare) that was detected using the ECL Western blotting Detection kit on Hyperfilm^{TM} (GE Healthcare).

Liquid Chromatography-Tandem Mass Spectrometry—Liquid chromatography-tandem mass spectrometry (LC-ESI-MS/MS) was performed on an Agilent Technologies (Santa Clara, CA) 1200 SL HPLC system connected to an AB SCIEX (Foster City, CA) 4000 QTrap mass spectrometer equipped with a turbo ion spray source. LC separation was carried out on an Atlantis T3 3-μm (2.1 × 150-mm) reversed phase column (Waters Corp., Milford, MA) at ambient temperature using a mobile phase consisting of 0.1% formic acid in water (Solvent A) and acetonitrile (Solvent B), respectively. The gradient employed was as follows: 0–2 min, 0% B; 2–10 min, linear

TABLE 1
Oligonucleotide primers used in RT-PCR assays
AFMID, arylformamidase; KYNU, kynureninase; KMO, kynurenine 3-hydroxylase; 3HAO, 3-hydroxyamino oxidase; KAT3, kynurenine aminotransferase.

Gene product	Primer sequences (5′ → 3′)	Product length	T_m
		bp	°C
IDO1-T1	GGGGGTCAGTGGAGTAGACA (forward) GCAGATTTCTAGCCACAAGGA (reverse)	173	60
IDO1-T2	TGCCTGGTTTTGAGGTTTTC (forward) GCAGATTTCTAGCCACAAGGA (reverse)	246	60
INDOL	CCTCATCCCTCCTTCCTTTC (forward) GGAGCAATTGCCTGGTATGT (reverse)	218	57
TDO	TGAATGCGCAAGAACTTCAG (forward) TTCCAGAACCGAGAACTGCT (reverse)	244	58
KYNU	CTTGGCCTTCAACCGAAA (forward) CAAAGCATTCATTAGAGCTATTTCTT (reverse)	200	57
KMO	TTCAATAAGCAGAGAAAACTTAAACAA (forward) TCACACCCTACAACAAGGTCA (reverse)	199	57
3HAO	CTAAGCCTGTTTGGGGACAG (forward) GGTTCCAGCAGGCACCAG (reverse)	197	60
AFMID	CCGCAGTGTCGTGTTTCTAC (forward) CTATGAGGGGCTCCAGGTC (reverse)	200	60
KAT3	GCTGCCAAGATGGTCTCTGT (forward) TTCCACTGGGAAAGGATTTTT (reverse)	200	57
GAPDH	GAAGACTGTGGATGGCCCCTC (forward) GTTGAGGGCAATGCCAGCCCC (reverse)	358	58

increase from 0 to 90% B; 10–12 min, hold at 90% B. Then the mobile phase was returned to 0% B, and the column was re-equilibrated with 0% B for 5 min. The flow rate was 400 μl/min. Injection volumes were 10 μl.

The 4000 QTrap mass spectrometer was operated in positive mode using turbo ion spray with gas 1, gas 2, and curtain gas set at 50, 50, and 10 arbitrary units, respectively. The source was heated to 500 °C. Quantitative determination was performed by multiple-reaction monitoring. All MS parameters were optimized by direct infusion, and the source parameters were optimized by flow injection. Data analysis was performed using Analyst version 1.5.1 (AB SCIEX).

Calibration curves were generated by serial dilution of 1 mM aqueous stock solutions of unlabeled Trp, kynurenine (KYN), kynurenic acid (KA), 3-hydroxykynurenine, xanthurenic acid, anthranilic acid, 3-hydroxyanthranilic acid, indole-3-acetic acid, melatonin and serotonin (Sigma-Aldrich) over a concentration range of 0.5–400 μM. To compensate for matrix effects, standard solutions were spiked with a ubiquitously ^{13}C isotope-labeled yeast extract (Silantes GmbH) as well as 0.1 μM melatonin-d_4 and 1.0 μM serotonin-d_4 creatinine sulfate complex from C/D/N Isotopes (Pointe-Claire, Canada). Standard calibration curves were plotted as the chromatographic peak area ratio *versus* the corresponding nominal concentration ratio. A $1/x$ weighted regression analysis was used to determine the slope, intercept, and coefficient of determination (r^2). Lower limits of quantitation ranged from 1 to 5 nM with the exception of tryptophan (0.1 μM), and the linear ranges extended from 500 to 3000 nM except for tryptophan (400 μM).

Measurement of Cytokine Levels—Commercially available mouse inflammation antibody arrays (RayBiotech, Inc., Norcross, GA) were used to detect cytokine expression. Caput epididymal protein extracts ($n = 3$) were treated as described by the supplier.

Measurement of Proteasome Activity and Ubiquitin Protein Conjugate Contents—To assess the peptidase activities associated with proteasomal activity, caput epididymal samples from WT and *Ido1*$^{-/-}$ mice were homogenized in 10 volumes of ice-cold 50 mM Tris-HCl buffer, pH 7.5, containing 250 mM sucrose, 10 mM ATP, 5 mM $MgCl_2$, 1 mM DTT, and protease inhibitors (10 μg/ml each of antipain, aprotinin, leupeptin, and pepstatin A and 20 μM PMSF) as described (13, 14). Proteasomes were isolated by three sequential centrifugations (13, 14). The final pellet was resuspended in 50 mM Tris-HCl, pH 7.5, containing 5 mM $MgCl_2$ and 20% glycerol. Protein content of these concentrates was determined according to Lowry *et al.* (15). Proteasome chymotrypsin-like, trypsin-like, and peptidyl-glutamyl peptide-hydrolyzing activities were determined by measuring the hydrolysis of the fluorogenic substrates succinyl-Leu-Leu-Val-Tyr-7-amido-4-methylcoumarin (LLVY-AMC), Boc-Leu-Arg-Arg-7-amido-4-methylcoumarin (LRR-AMC), and benzyloxycarbonyl-Leu-Leu-Glu-β-naphthylamide (LLE-bNa) (Sigma-Aldrich), respectively. Fifteen μl of concentrate were mixed with 60 μl of 50 mM Tris-HCl, pH 8.0, 10 mM $MgCl_2$, 1 mM DTT, 2 units of apyrase, and either 300 μM LLVY-AMC or 800 μM LRR-AMC and LLE-bNa, respectively. Reactions were performed with or without the proteasome inhibitor MG132 (40 μM; KCOM Group Plc, Hull, UK). Chymotrypsin- and trypsin-like activities were determined by measuring the accumulation of the fluorogenic cleavage product AMC by means of a fluorescence spectrometer FLX800 (BioTek, Colmar, France) over 45 min at excitation and emission wavelengths of 380 and 440 nm, respectively. Peptidyl-glutamyl peptide-hydrolyzing activity was determined by measuring the accumulation of the fluorogenic cleavage product (bNa) over 45 min at excitation and emission wavelengths of 340 and 450 nm, respectively. Proteasome activities were measured by calculating the difference between arbitrary fluorescence units recorded with or without MG132 in the reaction medium. The final data were corrected by the amount of protein in the reaction medium. The time course for the accumulation of AMC or bNa after hydrolysis of the substrate was analyzed by linear regression to calculate activities (*i.e.* the slopes of best fit of accumulated AMC or bNa *versus* time).

Accumulation of Ub protein conjugates in caput epididymal samples from WT and *Ido1*$^{-/-}$ mice was assessed by immuno-

blotting using the FK1 antibody (KCOM), which recognizes polyubiquitin chains. Samples were homogenized in ice-cold 5 mM Tris-HCl, pH 7.5, 5 mM EDTA, 1 mM PMSF, 0.25 mM N^{α}-*p*-tosyl-L-lysine chloromethyl ketone, 5 mM *N*-ethylmaleimide, 5 μg/ml leupeptin, and 5 μg/ml soybean trypsin inhibitor (13). Homogenates were centrifuged for 5 min (1500 × g, 4 °C). Supernatants were centrifuged again for 10 min (10,000 × *g*, 4 °C), and the resulting supernatants were ultracentrifuged for 3 h (100,000 × *g*, 4 °C). The final supernatants were stored at −80 °C until processed. The accumulation of Ub-protein conjugates was measured on proteins from this last supernatant. Protein concentration was determined as described (15). Twenty-five μg of protein were separated on 7.5% (w/v) acrylamide gels and transferred onto PVDF membranes. The FK1 antibody was used at a 1:1000 dilution. Signals were detected using the ECL+ detection kit (GE Healthcare) after exposition on Hyperfilm ECL (GE Healthcare), quantified using the Image J software, and normalized against the amount of protein determined by Ponceau Red staining to correct for uneven loading. [^{35}S]Methionine incorporation was used to assess the rate of protein synthesis in caput epididymides and was performed as originally described (16, 17).

Fertility and Spermatozoa Analyses—Five each of WT and *Ido1*$^{-/-}$ male mice, 6 or 12 months of age, were mated for 8 days with 2 BALB/c WT females. At the end of the 15-day reproductive period, males were removed, and females were housed in individual cages in order to follow eventual pregnancies and deliveries. Time to conceive and number of pups per litter were monitored. For sperm preparations, mice were killed by CO_2 asphyxiation. Epididymides were removed, divided into caput and caudal regions, and transferred to a small glass dish containing 1 ml of M2 medium (Sigma-Aldrich). To recover the spermatozoa, the caudae epididymides were repeatedly punctured with a 26-gauge needle. After 5 min of incubation to allow for sperm dispersal, these preparations were centrifuged at 500 × *g* for 5 min, and pellets were resuspended in 200 μl of M2. Eosin exclusion was used to assess sperm viability, whereas morphology was examined using the Shorr stain. The presence of leukocytes in cauda luminal fluid was assessed using a commercially available Leucoscreen™ kit as recommended by the supplier (FertiPro NV).

Statistical Analysis—Analysis of variance ANOVA 2 and Student's *t* tests were performed to determine the significance of differences between samples. *p* values of ≤0.05 were regarded as significant.

RESULTS

Tryptophan-catabolizing Enzyme Expression in WT and Ido1$^{-/-}$ *Mouse Caput Epididymis*—Immunocytochemical analysis revealed that IDO is expressed in WT BALB/c mice posterior to the initial segment S1 of the caput epididymis and ceases after the caput's most distal segment, S5 (Fig. 2*A*). IDO expression is maximal in S2–S4, and patchy in S5. IDO accumulates as a cytoplasmic protein in the epithelial cells of those segments. Fig. 2, *B* and *C*, shows that both known IDO transcripts (IDO mRNA1 and mRNA2; Ido1-T1 and Ido1-T2, respectively) are expressed in WT BALB/c caput epididymis and that they accumulate over a period of 25–30 days during postnatal ontogenesis until sexual maturity is reached and spermatozoa are released into the epididymal lumen. To verify that spermatozoa entering the epididymal tubule at sexual maturity could trigger IDO expression, we inhibited spermatogenesis by treating male mice aged 20 days with busulfan, which blocks germinal cell meiosis without affecting the secretory activity of Sertoli cells. Busulfan treatment significantly inhibited IDO expression at 30 DPN as compared with DMSO-treated as well as untreated controls (Fig. 2*C*). Other tryptophan-catabolizing enzymes, such as INDOL (also called IDO2 (18, 19)) and TDO (11), are expressed at much lower levels in the adult mouse caput epididymis (Fig. 2, *B* and *D*). The absence of IDO expression was not compensated by increased accumulation of TDO and INDOL transcripts in the *Ido1*$^{-/-}$ animals (Fig. 2*D*). In fact, these transcripts were even less abundant in *Ido1*$^{-/-}$ as compared with the WT controls.

Evaluation of Tryptophan Catabolites along the IDO Pathway in WT and Ido1$^{-/-}$ *BALB/c Mice*—Using semiquantitative RT-PCR, we measured the expression of the first five enzymes of the IDO pathway in total RNA extracts of caput epididymal tissue (Fig. 2*E*). It appears that the mouse caput epididymis expresses some of the major enzymes of the kynurenine pathway downstream of IDO. A semiquantitative comparison of the different amplifications carried out on a pool of WT caput epididymal cDNAs ($n = 6$) indicated that arylformamidase and kynurenine aminotransferase were the most abundant enzymes of the IDO pathway in mouse caput epididymis aside from IDO itself. Kynureninase and kynurenine 3-hydroxylase were expressed at much lower levels.

LC-ESI-MS/MS was used to measure the concentrations of various tryptophan-derived metabolites in caput epididymal extracts as well as in sera from WT and *Ido1*$^{-/-}$ animals (Table 2 and Fig. 3*A*). In agreement with the constitutive expression of IDO in the mouse caput epididymis, KYN was highly abundant in caput extracts of WT animals. Downstream of KYN, KA and 3-hydroxykynurenine (HK) were the second and third most abundant kynurenine species, respectively, in WT caput epididymis. Anthranilic acid, 3-hydroxyanthranilic acid, and xanthurenic acid were also present in WT caput extracts but at lower concentrations that were similar to systemic levels (Fig. 3). The concentrations of quinolinic acid and nicotinic acid in both caput epididymis and serum samples were below the lower limits of quantitation of the MS method employed.

Identical measurements of Trp and its metabolites were performed in *Ido1*$^{-/-}$ animals. As illustrated in Fig. 3*A*, we observed a dramatic decrease in both KYN (>100 times less) and KA (about 50 times less) levels in caput epididymal extracts of *Ido*$^{-/-}$ animals. The caput epididymal levels of HK, anthranilic acid, 3-hydroxyanthranilic acid, and xanthurenic acid were also reduced in the *Ido*$^{-/-}$ animals but to a lesser extent.

Does the Absence of IDO Activity Change the Inflammatory Status of the Caput Epididymis?—The KYN/Trp ratio is commonly used to evaluate IDO activity and, by extension, the immunosuppressive status of a given tissue or biological fluid (20). Fig. 4*A* shows that the KYN/Trp ratio in WT caput epididymis is about 38-fold higher than that in serum, suggesting that in adult WT mice, the caput epididymis is in an immunosuppressed state. In the *Ido*$^{-/-}$ animals, the situation was reversed,

with a caput KYN/Trp ratio not much different from serum (0.008 and 0.004, respectively).

To evaluate the inflammatory status of the caput epididymis in WT and *Ido1*$^{-/-}$ animals, we measured the levels of various inflammatory cytokines by the use of mouse inflammation antibody arrays from RayBiotech. As shown in Fig. 4*B*, levels of some selected inflammatory cytokines were significantly higher in *Ido1*$^{-/-}$ than in WT animals, attesting to an overall more pronounced or at least different inflammatory state of the caput territory in the absence of IDO. In agreement with the hypoth-

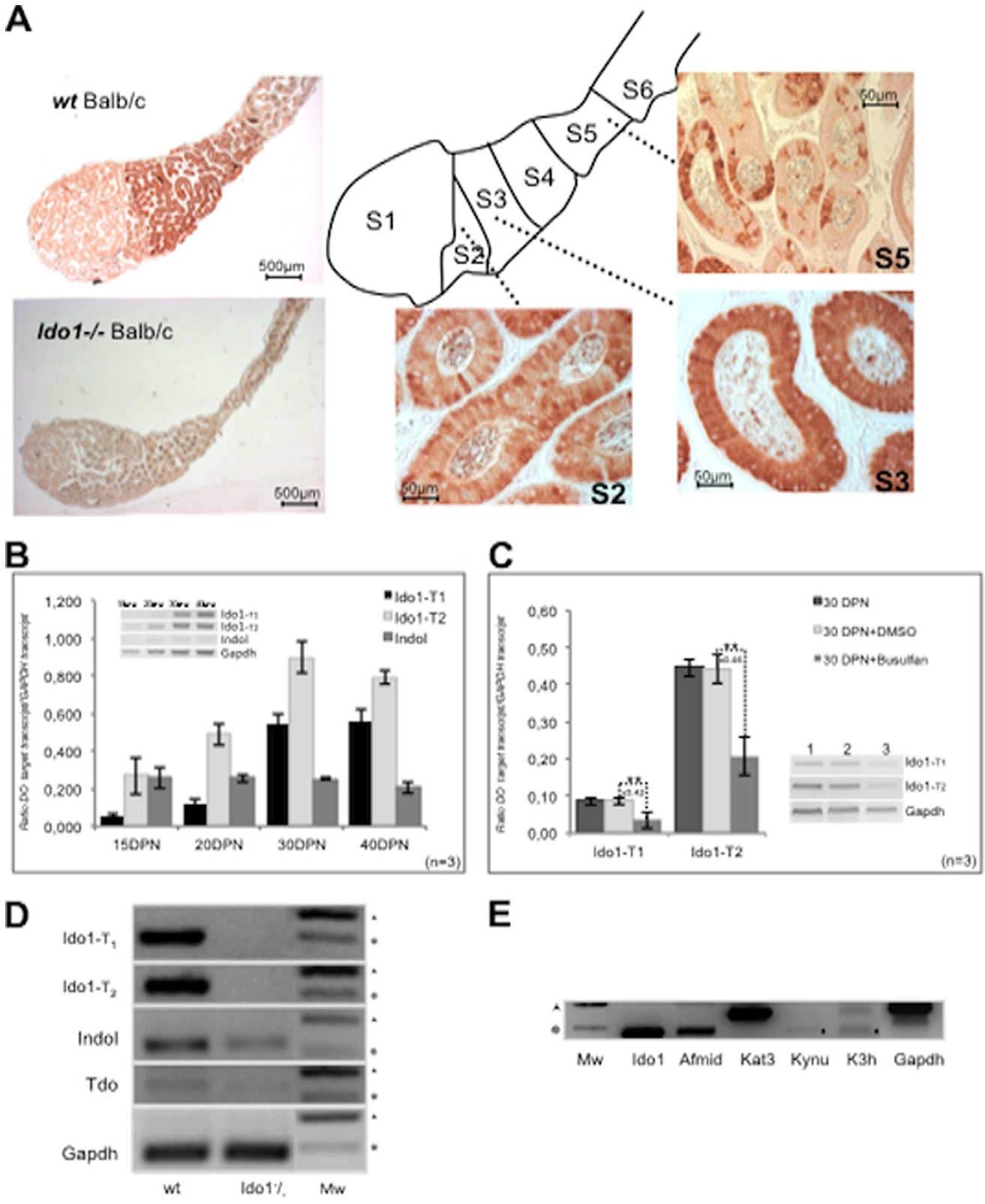

TABLE 2

Concentrations of Trp and Trp catabolites along the kynurenine pathway in caput epididymis extracts and whole sera of WT and *Ido1*$^{-/-}$ animals

Mean concentrations are given in nmol/g for all analytes except tryptophan, where the concentrations are in μmol/g. S.E. values (n = 3) are shown in italic type. Concentrations in sera are given in nM except tryptophan, where the concentrations are in μM. Numbers with plus and minus symbols preceding indicate positive (+) or negative (−) -fold differences between WT and *Ido1*−/− animals. Kyn, kynurenine; AA, anthranilic acid; HAA, 3-hydroxyanthranilic acid; XA, xanthurenic acid.

	Trp	Kyn	KA	HK	AA	HAA	XA
Caput epididymidis							
WT							
Mean	70.91	80547.23	1241.21	688.91	103.18	52.89	20.62
S.E.	*1.14*	*12704.51*	*54.51*	*37.40*	*7.05*	*4.12*	*6.02*
Ido1−/−							
Mean	174.03	680.06	25.30	198.17	70.14	36.98	12.87
S.E.	*9.33*	*60.38*	*0.66*	*24.70*	*9.39*	*2.10*	*1.13*
Ido1−/− *versus* WT (-fold difference)	+2.45	−118.44	−49.06	−3.48	−1.47	−1.43	−1.60
Serum							
WT							
Mean	50.68	1467.65	105.98	49.05	78.43	24.09	62.38
S.E	*7.62*	*356.11*	*43.52*	*27.52*	*4.58*	*4.97*	*12.40*
Ido1$^{-/-}$							
Mean	53.66	420.73	52.60	24.01	64.28	18.57	37.36
S.E	*10.15*	*79.65*	*9.99*	*13.17*	*2.15*	*2.91*	*1.60*
Ido1−/− *versus* WT (-fold difference)	+1.06	−3.49	−2.01	−2.04	−1.22	−1.30	−1.67

esis that outside the caput epididymis other tryptophan-catabolizing enzymes (TDO presumably) could compensate for the lack of IDO in *Ido1*$^{-/-}$ animals, we show in Fig. 4*C* that none of the cytokines found up-regulated in the caput extracts are statistically different in the sera of *Ido1*$^{-/-}$ animals as compared with WT. Confirming the peculiar inflammatory behavior of the caput epididymis territory, the three selected cytokines that did not change in WT *versus Ido1*$^{-/-}$ caput (*i.e.* IL-4, MCP1, and MCSF) were found down-regulated in the serum samples of WT animals *versus Ido1*$^{-/-}$ (Fig. 4, *B* and *C*).

Does the Absence of IDO Activity Increase the Availability of Trp for the Other Trp-dependent Pathways?—The absence of IDO expression and, consequently, of Trp consumption along the kynurenine pathway results in a 2.5-fold increase in caput epididymal Trp concentration (Fig. 5*A*). Because Trp can be used for the generation of other Trp derivatives such as indole-3-acetic acid, serotonin, and melatonin (see Fig. 1), we investigated whether there was any increase in the abundance of these metabolites in caput epididymal extracts of *Ido1*$^{-/-}$ animals. As shown in Table 3, the observed increase in Trp concentration in caput epididymal extracts of *Ido1*$^{-/-}$ animals had no significant impact on the abundance of indole-3-acetic acid, serotonin, and melatonin.

The major utilization route of amino acids is along the protein synthesis pathway to support the production of proteins (see Fig. 1). Considering that Trp is often the rate-limiting amino acid in protein synthesis, we asked whether the increase in Trp concentration in caput epididymal extracts of *Ido1*$^{-/-}$ animals could lead to an increase in protein synthesis and, consequently, to an increased caput protein content. To that end, we compared the protein contents of WT and *Ido1*$^{-/-}$ caput epididymal samples and observed, in relation to organ weight, significantly greater amounts of protein in caput epididymal extracts of *Ido1*$^{-/-}$ animals as compared with WT controls (Fig. 5*B*). This increase in protein content was not due to an enlargement of the caput epididymis in *Ido*$^{-/-}$ animals, because the mean weights of caput tissues were not statistically different in *Ido1*$^{-/-}$ and WT animals. It was also not the consequence of increased cell content or proliferation as measured via histological and immunocytological approaches (DAPI staining and Ki67 or PCNA antibody; data not shown).

The Higher Protein Content of Ido1$^{-/-}$ *Caput Epididymis Extracts Is Due to Decreased Protein Degradation*—Cellular or tissue protein content is a balance between protein synthesis and protein degradation. To clarify the origin of the increased protein content in caput extracts from *Ido1*$^{-/-}$ animals, we monitored both. Regarding protein synthesis, an excess of amino acid availability is known to activate the mTOR pathway, ultimately leading to an increase in protein synthesis (21–23). To monitor whether the increase in Trp

FIGURE 2. **IDO expression in the mouse epididymis.** *A*, immunohistochemical localization of IDO protein in a longitudinal section (*top left panel*) of a 6-month-old WT BALB/c caput epididymis. The *top middle panel* schematizes the various segments separated by connective septa found in the caput. *Panels S2*, *S3*, and *S5* show the intracellular epithelial localization of IDO in the various segments as well as its patchy appearance (especially in segment *S5*). The *bottom left panel* illustrates the absence of IDO in a longitudinal section of a caput epididymis from *Ido1*$^{-/-}$ male mice 6 months of age. *B*, semiquantitative RT-PCR amplifications of the two known IDO transcripts (IDO1-T1 and IDO1-T2), as well as the INDOL transcript, in caput epididymal total RNA extracts from 6-month-old male mice (n = 3) during postnatal ontogenesis at 15, 20, 30, and 40 days of life. Transcript levels in the *y axis* are given in arbitrary units representing the transcript level normalized to GAPDH expression. A representative amplification is shown as an *inset*. *C*, semiquantitative RT-PCR amplifications of the two known IDO transcripts in untreated (*30 DPN*), vehicle-treated (*30 DPN + DMSO*), and busulfan-treated (*30 DPN + Busulfan*) animals (*lanes 1–3*, respectively, in the representative Western blot presented as an *inset*). Transcript levels in the *y axis* are given in arbitrary units representing the transcript level normalized to GAPDH expression. *D*, representative RT-PCR amplifications of IDO-T1, IDO-T2, INDOL, and TDO transcripts in WT and *Ido1*$^{-/-}$ caput epididymis total RNA extracts showing the complete loss of both IDO transcripts in the caput of Ido1$^{-/-}$ animals. Please note that INDOL and TDO mRNA are not up-regulated in parallel. *Boldface asterisks* on the *right* indicate the 400 and 200 bp bands of the molecular weight marker run in *lane Mw*. *E*, RT-PCR analysis of the expression of the various enzymes (IDO (*Ido1*), arylformamidase (*Afmid*), kynurenine aminotransferase (*Kat3*), kynureninase (*Kynu*), and kynurenine 3-hydroxylase (*K3h*)) involved in the kynurenine pathway (see Fig. 1) in the caput epididymis of WT BALB/c mice along with the amplification of a GAPDH control. Each amplification was performed on pooled cDNA generated from caput epididymal tissues collected from 6 animals (aged 6 months). *Boldface asterisks* on the *right* indicate the 400 and 200 bp bands of the molecular weight marker run in *lane Mw*. *Error bars*, S.D.

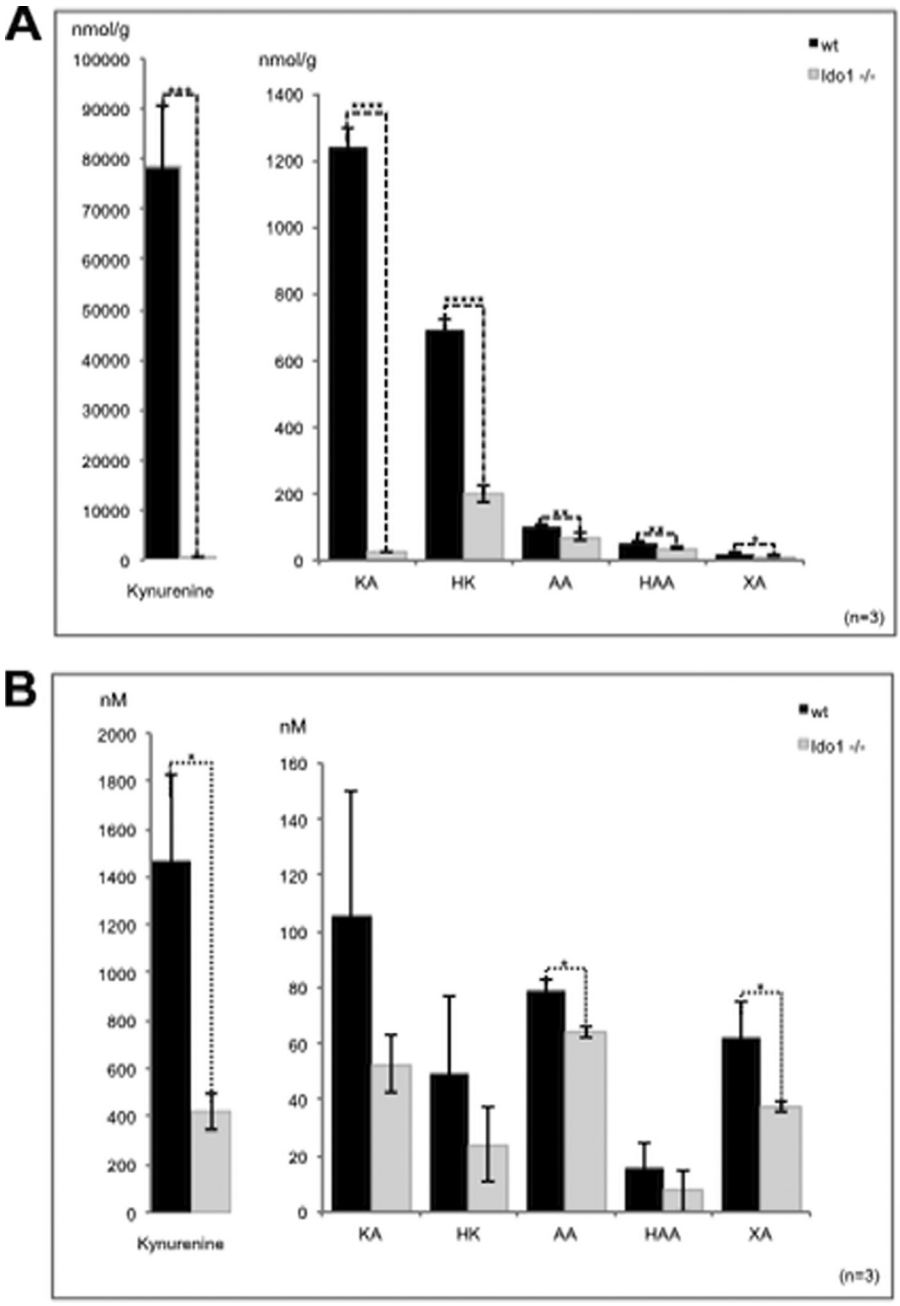

FIGURE 3. **Concentrations of Trp and Trp catabolites along the kynurenine pathway in caput epididymal extracts and whole sera of WT and *Ido*$^{-/-}$ animals.** Histograms illustrate the recorded differences in kynurenine concentrations in caput epididymal extracts (*A*) and sera (*B*) from 6-month-old WT and *Ido1*$^{-/-}$ animals. *KA*, kynurenic acid; *KH*, hydroxykynurenic acid; *AA*, anthranilic acid; *HAA*, hydroxyanthranilic acid. *, $p \leq 0.5$; **, $p \leq 0.01$; ***, $p \leq 0.001$; ****, $p \leq 0.0001$; *****, $p \leq 0.00001$. *Error bars*, S.E.

observed in caput epididymal extracts of *Ido*$^{-/-}$ animals stimulates protein synthesis via the mTOR pathway, we performed Western blot analyses using antibodies directed against phosphorylated mTOR and one of its direct targets, the p70S6 kinase. Fig. 5*C* shows that neither kinase is activated in caput epididymal extracts of both *Ido1*$^{-/-}$ and WT animals. To confirm that increased protein synthesis was not responsible for the higher protein content of *Ido1*$^{-/-}$ caput tissues, we have carried out [^{35}S]methionine incorporation assays in organotypic cultures of caput epidiymides from WT and *Ido1*$^{-/-}$ animals. Data presented in Fig. 5*D* attest that the rate of the amino acid tracer incorporation is not statistically different between WT and *Ido1*$^{-/-}$ animals.

Because pathways leading to increased protein synthesis were not enhanced in *Ido*$^{-/-}$ animals, we hypothesized that the higher protein content was due to a decrease in protein degradation. The two major cellular pathways responsible for protein degradation are the ubiquitin/proteasome system and the lysosomal compartment. To evaluate the activity of the ubiquitin/proteasome system in caput epididymal samples, we first monitored the three major proteolytic activities associated with the 26 S proteasome. As shown in Fig. 6*A*, chymotrypsin-like, tryp-

A

	CAPUT KYN/Trp	SERUM KYN/Trp	caput vs serum
WT	1.14	0.03	38
Ido-/-	0.004	0.008	0.5
IDO-/- vs WT	-285	-3.75	

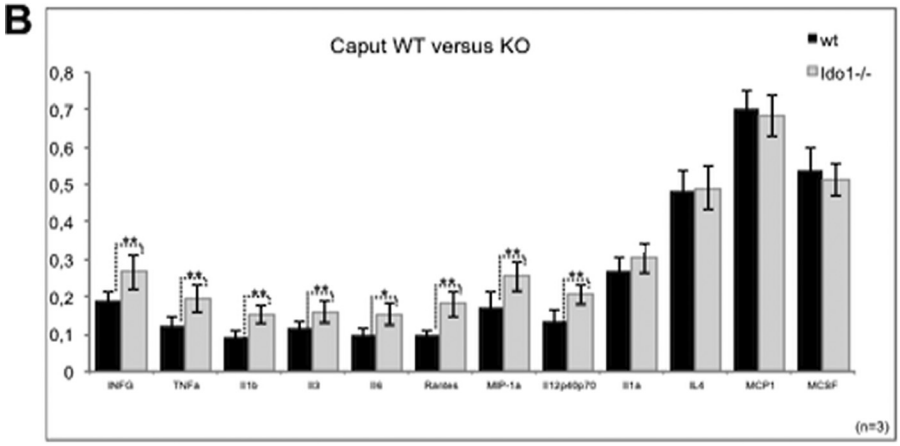

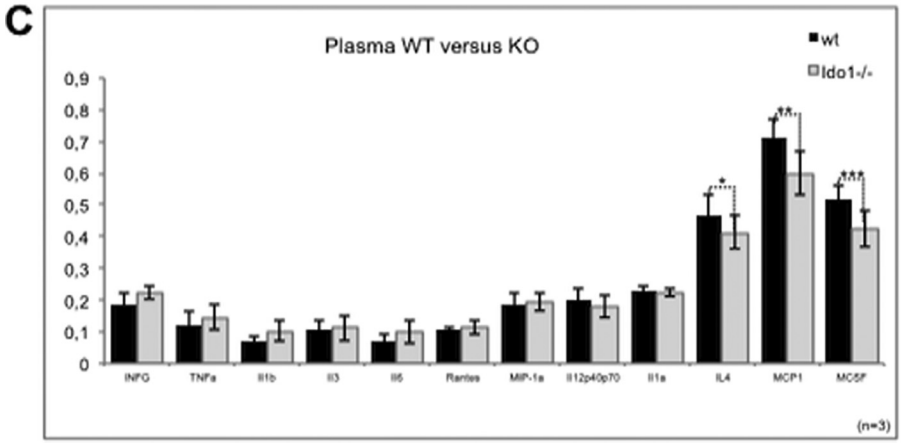

FIGURE 4. **Analysis of the inflammatory status of the epididymis.** *A*, Kyn/Trp ratio in caput epididymis and serum from 6-month-old WT and *Ido1*$^{-/-}$ animals. -Fold differences are indicated on the *right side* of the *table* (caput *versus* serum) and at the *bottom* of the *table* (*Ido1*$^{-/-}$ *versus* WT). *B* and *C*, histograms show the levels of various inflammatory cytokines (INF-γ, TNF-α (*TNFa*), interleukin-1β (*IL1b*), IL-3 (*Il3*), interleukin-6 (*Il6*), regulated on activation normal T cell expressed and secreted (*RANTES*), interleukin-12p40p70 (*Il12p40p70*), interleukin 4 (*Il4*), monocyte chemoattracting protein 1 (*MCP1*), and macrophage/monocyte colony-stimulating factor (*MCSF*)) in caput epididymal extracts (*B*) and sera (*C*) from 6-month-old WT and *Ido1*$^{-/-}$ animals. *, $p \leq 0.5$; **, $p \leq 0.01$; ***, $p \leq 0.001$. *Error bars*, S.E.

sin-like, and peptidyl-glutamyl peptide-hydrolyzing activities were decreased by ~40% in *Ido1*$^{-/-}$ caput epididymal samples as compared with WT ($p < 0.001$). In contrast to proteasomal activities, poly-Ub conjugates remained unchanged in *Ido1*$^{-/-}$ *versus* WT caput epididymal samples (Fig. 6*B*).

The Lysosomal/Autophagic Pathway Is Locally Activated in the Caput Epididymis of Ido1$^{-/-}$ *Animals*—Next we asked whether the lysosomal pathway would back up the failing proteasomal pathway in the caput epididymis of *Ido*$^{-/-}$ animals. The lysosomal pathway is a complex pathway that uses several parallel routes, including macroautophagy, microautophagy, and chaperone-mediated autophagy. In Fig. 6*C*, we show that these autophagic processes were indeed triggered in the caput epididymis of *Ido1*$^{-/-}$ animals, because beclin-1/ATG6, one of the early ATG (autophagy-related) gene products (reviewed in Ref. 24), was clearly up-regulated in caput epididymal samples of *Ido1*$^{-/-}$ animals as compared with WT.

Because endosomal/lysosomal autophagy is often reflected in cell phenotypic modifications, we used photon and electron microscopy to compare WT and *Ido*$^{-/-}$ caput epididymal tissues. As shown in Fig. 7, *A–D*, IDO deficiency led to a caput segment S2-localized phenotype that was characterized by cytoplasmic vesicles, which were not visible in WT caput sections. Transmission electron microscopy of segment S2 of the caput epididymis in *Ido1*$^{-/-}$ animals (Fig. 7, *E–G*) revealed an elevated level of multilamellar/multivesicular bodies as compared with WT sections. Such structures are known autophagic features (25).

IDO Deficiency Affects Sperm Number and Morphology but Not Overall Fertility—To study the impact of IDO deficiency on reproductive competence, *Ido1*$^{-/-}$ males were mated

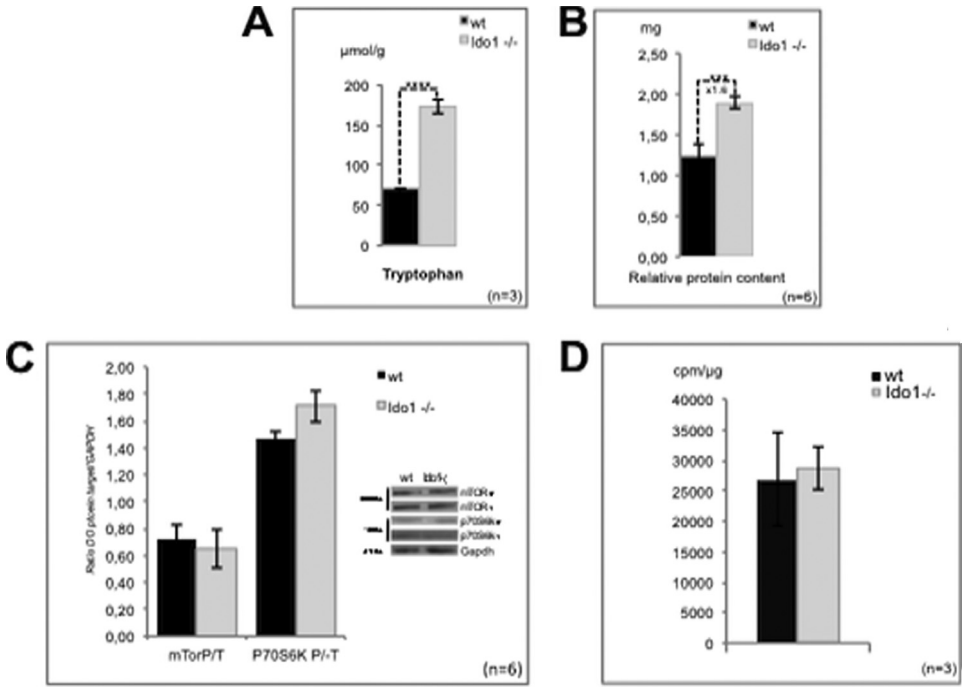

FIGURE 5. **IDO deficiency leads to Trp accumulation and higher protein content in caput epididymal extracts of *Ido1*$^{-/-}$ animals.** *A*, histogram of Trp concentrations in caput epididymal extracts from 6-month-old *Ido1*$^{-/-}$ and WT mice, respectively ($n = 3$ each). *B*, evaluation of caput epididymal total protein content relative to organ weight from 6-month-old WT and *Ido1*$^{-/-}$ mice ($n = 6$ each). Mean weights of WT caput tissues were not found to be statistically different from that of *Ido*$^{-/-}$ caput tissues and were 20.17 ± 0.87 and 19,37 ± 1.87 mg, respectively. *C*, a representative Western blot showing the levels of total mTOR (*mTOR-T*) or the activated phosphorylated form of mTOR (*mTOR-P*) as well as of the total p70S6K (*p70S6K-T*) and the activated phosphorylated form of p70S6K (*p70S6K-P*) is shown in the *left panel*. GAPDH immunodetection was used as an internal standard. Histograms in the *right panel* show a comparative quantitative analysis of phosphorylated mTOR/total mTOR and phosphorylated p70S6K/total p70S6K between caput epididymis protein extracts from 6-month-old WT and *Ido1*$^{-/-}$ mice ($n = 6$ each). *D*, [^{35}S]methionine incorporation in organotypic cultures of caput epididymis from WT and *Ido*$^{-/-}$ animals ($n = 3$ each). *Error bars*, S.E.

TABLE 3

Concentrations in nM/kg of other non-kynurenine Trp catabolites in caput epididymis extracts

For non-kynurenine Trp derivatives (namely indoxyl acetic acid (IAA), serotonin, and melatonin), mean concentrations are given in nmol/g. S.E. values ($n = 3$) are shown in italic type. Numbers with plus and minus symbols preceding indicate positive (+) or negative (−) -fold differences between WT and *Ido1*$^{-/-}$ animals.

	IAA	Serotonin	Melatonin
WT			
Mean	133.75	1708.40	9.80
S.E.	*9.18*	*355.20*	*0.69*
***Ido1*−/−**			
Mean	140.92	2382.83	11.07
S.E.	*16.90*	*641.70*	*0.53*
Ido1−/− *versus* WT (-fold difference)	+1.05	+1.39	+1.13

with WT BALB/c female mice. Mating was conducted using female mice at optimal reproductive age (3 months) and groups of $n = 5$ each WT or *Ido1*$^{-/-}$ males 6 and 12 months of age, respectively. No changes in mating behavior were noticed with any of the animal groups tested. Both 6- and 12-month-old male *Ido1*$^{-/-}$ mice showed normal fertility, with litter sizes of 6.6 ± 0.7 and 6.1 ± 1.0 pups, respectively (Fig. 8*A*). In comparison, the respective litter sizes in WT mice were 5.4 ± 1.5 and 6.6 ± 0.6 pups. Time to gestation was also comparable (data not shown). These data suggested that at least up to an age of 1 year, IDO deficiency had no deleterious impact on the fertilization competence of *Ido1*$^{-/-}$ males. Nevertheless, we noticed some interesting differences between WT and *Ido1*$^{-/-}$ males. First, the cauda epididymal sperm counts were nearly twice as high in *Ido1*$^{-/-}$ animals as compared with WT animals (Fig. 8*B*). In the absence of a difference in testis weight (Fig. 8*C*), the increase in sperm count was unlikely to be due to an increase in testicular spermatogenesis. Sperm viability and motility were also assessed, and we found that the percentages of dead and immotile spermatozoa were only slightly higher in cauda preparations from *Ido1*$^{-/-}$ as compared with WT animals (not shown). However, we did notice a significant increase in the proportion of spermatozoa exhibiting abnormal morphology in the *Ido1*$^{-/-}$ animals *versus* WT animals, including pinhead, giant head, hairpin, and kite spermatozoa (Fig. 8*E*). Finally, we observed that the concomitant increase in sperm number and decrease in sperm quality were associated with a significant decrease in the leukocyte count in the caudal epididymal fluid of *Ido1*$^{-/-}$ animals (Fig. 8*D*).

DISCUSSION

The IDO Pathway and Immunosuppression in the Mouse Caput Epididymis—In accordance with previous studies (11, 26, 27), IDO is strongly expressed in the mouse caput epididymis, whereas TDO is not. The expression of both known IDO transcripts increased gradually during postnatal development of the caput epididymis and reached a maximum at the time of sexual maturity. IDO-mRNA2 appears to be the more abundant IDO transcript in the mouse caput epididymis. We have shown that INDOL, which is a mammalian IDO homologue located in close proximity on the same mouse chromosome as the result of an IDO gene duplication event (26, 27), is also

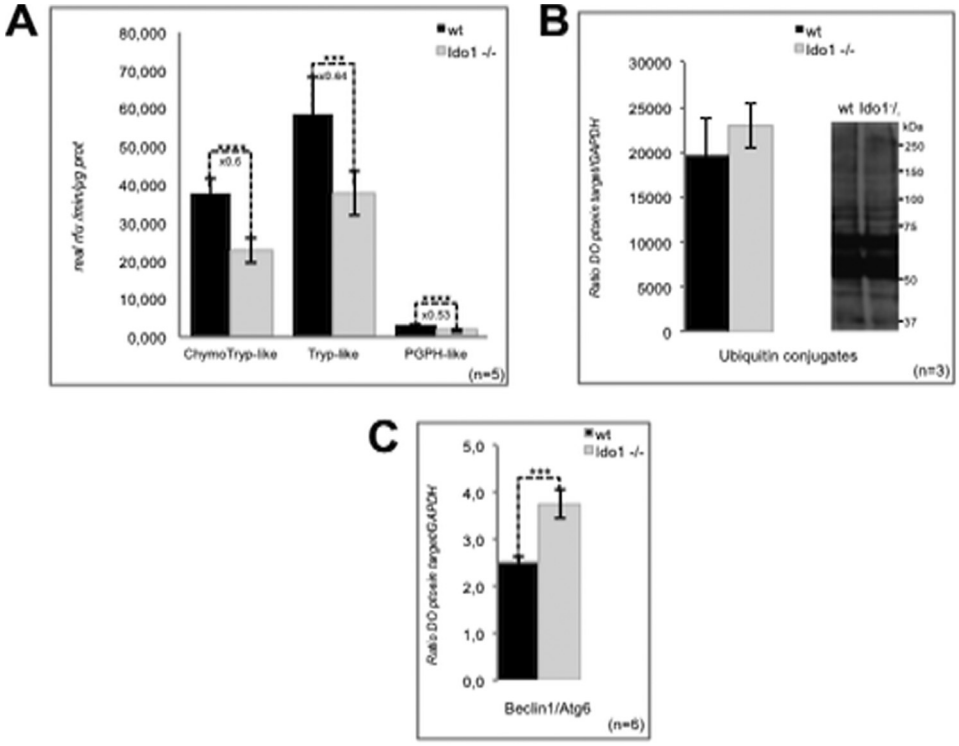

FIGURE 6. **Proteasomal protein degradation and autophagy induction in WT and *Ido1*$^{-/-}$ caput epididymal protein extracts.** *A*, histograms show the three major peptidase activities of the proteasome (chymotrypsin-like (*ChymoTrp-like*), trypsin-like (*Tryp-like*), and peptidyl-glutamyl peptide-hydrolyzing (*PGPH-like*)) in caput epididymal protein extracts from 6-month-old WT and *Ido1*$^{-/-}$ mice (*left*). The *numbers above* the *columns* give the -fold difference recorded. *B*, histogram presents the level of polyubiquitinated proteins found in caput protein extracts from 6-month-old WT and *Ido1*$^{-/-}$ animals (a representative Western blot is shown on the *right* to show that neither the intensity nor the banding pattern changes when WT extracts are compared with *Ido*$^{-/-}$ extracts). *C*, histogram shows a quantitative analysis of beclin-1/ATG6 (an early autophagy marker) in 6-month-old WT *versus Ido1*$^{-/-}$ mouse caput epididymal protein extracts ($n = 6$ each). ***, $p \leq 0.001$; ****, $p \leq 0.0001$. Data are expressed in cpm/μg of protein. *Error bars*, S.E.

expressed in the mouse caput epididymis, albeit at a much lower level. Contrary to IDO transcripts, accumulation of INDOL transcripts does not change during postnatal ontogeny of epididymal tissue. Busulfan treatment that stops spermatogenesis without affecting Sertoli cell functions shows that the epididymal accumulation of IDO transcripts is greatly reduced, suggesting that spermatozoa entering the epididymal duct trigger/sustain IDO expression. In the *Ido1*$^{-/-}$ knock-out, both IDO transcripts are lost in the epididymis. This IDO deficiency is not compensated for at the transcriptional level by an increased accumulation of INDOL and/or TDO transcripts. Accordingly, KYN production is dramatically reduced in *Ido1*$^{-/-}$ *versus* WT caput epididymal samples. These observations prove that IDO is the major kynurenine contributor in the mouse caput epididymis. Furthermore, the preferential localization of the enzymes TDO and INDOL on spermatozoa transiting the caput epididymis (11, 18, 19) suggests that Trp catabolism via IDO is essentially an epididymal epithelial phenomenon.

The strong constitutive expression of IDO in the mouse epididymis is accompanied by the generation of KYN, HK, and KA. Recent data have suggested that metabolites of the IDO pathway contribute to the generation of a tolerogenic state against foreign cells, including tumors and the fetal allograph (28, 29). In the case of KYN, this is achieved through the suppression of T-cell proliferation (30, 31). Less is known about KA and HK. The former may play a complementary role to KYN by reducing the secretion of proinflammatory cytokines, such as TNF-α and INF-γ (32).

A similar immunosuppressive role can be ascribed to IDO in the epididymis. Spermatozoa are generated long after immunological tolerance has been established, and for this reason, they are potentially immunogenic. In the testes, immune recognition is prevented by the blood-testis barrier, which physically shields postmeiotic germ cells from the immune system. Similarly, the epididymis is an immunologically privileged site that does not mount an autoimmune response against spermatozoa, although millions of these foreign cells are continually passing through its lumen. This is a delicate balancing act, for although tolerance is expressed toward spermatozoa in the epididymal lumen, full immunological competence is retained in the subepithelial compartment (33). IDO-dependent reduction in Trp levels in concert with the production of immunosuppressive kynurenines (KYN and KA) along with the blood-epididymis barrier formed by the epididymal epithelium may create the requisite tolerogenic state. This interpretation is somehow supported by the up-regulation of inflammatory cytokines (both pro- and anti-inflammatory) observed in the epididymides of *Ido1*$^{-/-}$ knock-out mice. The participation of IDO in establishing an immunosuppressive state around spermatozoa is also supported by the observation that IDO expression is triggered by spermatozoa entering the epididymis tubule at sexual maturity, as shown by the data obtained after busulfan treatment of young male mice. We hypothesize that in the absence of IDO

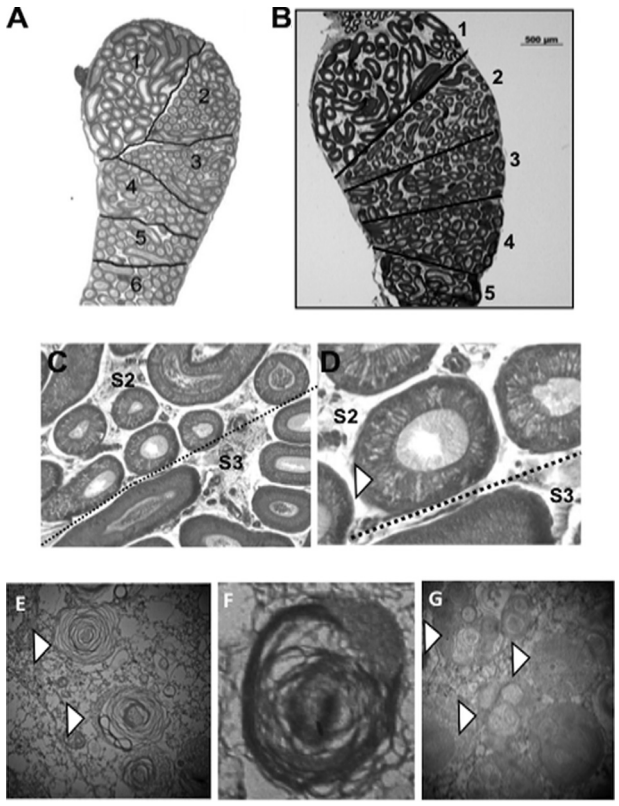

FIGURE 7. **IDO deficiency provokes a caput epididymal regionalized phenotype.** *A* and *B* show longitudinal caput epididymal sections of a WT and an *Ido1*$^{-/-}$ 6-month-old male mouse, respectively. In both *panels*, connective septa separating the various caput segments are *highlighted* (*dark black lines*). Note the weak staining of the caput segment S2 area in the *Ido1*$^{-/-}$ animal compared with WT. *C* and *D* show higher magnifications of caput epididymal tubules at the S2/S3 junction from an *Ido1*$^{-/-}$ animal (aged 6 months). Note the presence of numerous bright vesicles (*white arrowhead*) within the epithelium of S2 tubules. *E–G* show typical autophagic features revealed by transmission electron micrographs in caput segment S2 of an *Ido1*$^{-/-}$ animal. An example of multilamellar vesicles (*white arrowhead*) is magnified in *E* and *F* (magnification, ×40,000 in *E* and ×50,000 in *F*). An example of plurivesicular structures (*white arrowhead*) is shown in *G* (magnification, ×15,000).

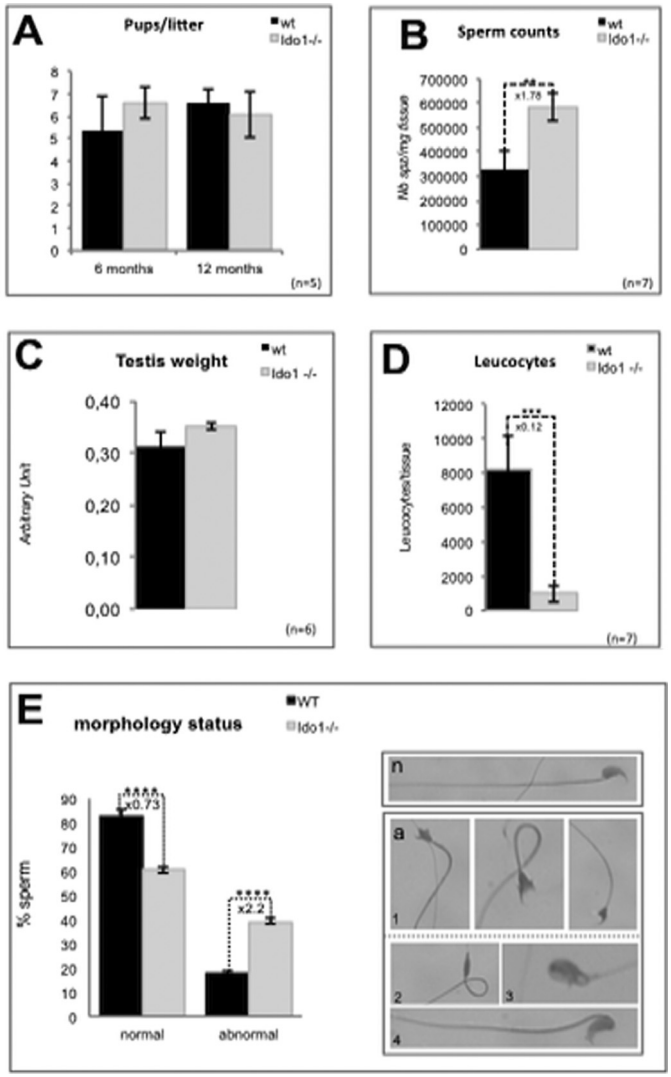

FIGURE 8. **Evaluation of fertility/spermatozoa parameters of *Ido*$^{-/-}$ males *versus* WT males.** *A*, histograms show the number of pups obtained when WT or *Ido*$^{-/-}$ male mice (either 6 or 12 months old) were mated with WT female mice (3 months old) of proven fertility ($n = 5$ each). *B*, histogram shows numbers of spermatozoa found in the caudae epididymides of 6-month-old WT and *Ido*$^{-/-}$ animals ($n = 7$ each). *C*, histogram shows the testis weights (relative to body weights) of WT *versus* *Ido*$^{-/-}$ animals (6 months old). The unit given in the *y* axis has been arbitrarily multiplied by 1000. *D*, histogram shows the leukocyte counts in cauda epididymal fluids of 6-month-old WT and *Ido*$^{-/-}$ animals ($n = 7$ each). *E*, histograms show the percentage of morphologically abnormal spermatozoa as revealed by Schorr staining in WT or *Ido*$^{-/-}$ male mice (WT, $n = 4$; *Ido*$^{-/-}$, $n = 5$). The *photograph panel* on the *right* shows an example of normal spermatozoa (*n*) and various abnormal (*a*) situations, including spermatozoa exhibiting kite head (*1*), pinhead (*2*), giant head (*3*), and hairpin (*4*) sperm that were found to be more numerous in *Ido*$^{-/-}$ *versus* WT male mice. **, $p \leq 0.01$; ***, $p \leq 0.001$; ****, $p \leq 0.0001$. *Error bars*, S.E.

expression and its associated tolerogenic effect, spermatozoa entering the tubule are likely to exacerbate the local inflammatory situation. However, we think that a new equilibrium is found in order to preserve the situation of immune tolerance toward spermatozoa, which may explain why the cytokine increase is minor and why it concerns both pro- and anti-inflammatory cytokines. This *in fine* might result in a diminution of the leukocyte population infiltrating the epididymis tubule. Several very recent papers have brought forward the idea that the classical Th1/Th2 balancing act in regulating the immune response in such immune privileged settings is not that simple (34–36).

The IDO Pathway and Changes in Protein Processing—The absence of IDO activity in the caput epididymis of *Ido1*$^{-/-}$ animals does not only nearly abolish KYN synthesis; it also leads to a 2.5-fold increase in the concentration of Trp. This was only observed in epididymal samples. In serum, Trp concentrations were quite similar in both WT and *Ido1*$^{-/-}$ genetic backgrounds, most likely because of TDO compensation. This reinforces the idea that Trp catabolism along the KYN pathway in the mouse caput epididymis is essentially driven by IDO and that other Trp-catabolizing enzymes do not compensate for IDO loss of function in this tissue. The fact that Trp concentrations were dramatically increased in caput epididymal tissues of *Ido1*$^{-/-}$ mice also suggests that Trp is not a rate-limiting amino acid in this tissue, although it is often the least abundant of the essential amino acids. Concordantly, we show here that the increase in *Ido*1$^{-/-}$ caput epididymal Trp content is not accompanied by significantly elevated concentrations of the non-kynurenine Trp derivatives indole-3-acetic acid, serotonin, and melatonin. However, *Ido1*$^{-/-}$ animals possessed a

higher caput epididymal protein content than WT animals. This was not due to an increase in protein synthesis but rather due to a decrease in protein catabolism mediated by a defective proteasome function.

Amino acid-mediated inhibition of protein catabolism has already been reported in liver and muscle cell extracts (37). It was shown that of all amino acids investigated, an excess of Trp was the most effective in impairing proteasomal activity. The competitive nature of this inhibition allowed the authors to suggest that it was triggered by a relative abundance of intracellular amino acids (37). We hypothesize that this situation pertains in the caput epididymis of *Ido1*$^{-/-}$ animals, where the elevated Trp content mediates an inhibition of proteasomal activity. We also show that the observed proteasome inhibition is not accompanied by an accumulation of ubiquitinated proteins in *Ido1*$^{-/-}$ caput epididymal protein extracts. This suggests that the ubiquitination rate either is very low or has been adjusted to avoid the otherwise deleterious accumulation of ubiquitinated protein aggregates that would drive cellular stress responses, eventually leading to apoptotic cell death (38). It is interesting to note that the literature also reports that proteasome inhibition may be one way that cells ameliorate an inflammatory situation and minimize autoimmunity (39, 40). In light of these findings, it is possible that the suppression of proteasome activity is an adaptive response on the part of the epididymis, designed to maintain a local tolerogenic environment toward spermatozoa in the face of a precipitous loss of IDO activity in the *Ido1*$^{-/-}$ animals.

Intracellular protein degradation is not solely ensured by the ubiquitin/proteasome system. It is also achieved by the lysosomal pathway through autophagic processes. Depending on the cell type and the nature of the stimulus, lysosomal and proteasomal protein degradation may work hand in hand and compensate for each other (41). We provide evidence that in the caput epididymis of *Ido1*$^{-/-}$ animals, autophagic processes might be increased to compensate for the deficient proteasomal pathway. In support of this hypothesis, we show that beclin-1/ATG6, one of the early ATG genes, is up-regulated in *Ido1*$^{-/-}$ caput epididymal protein extracts. Beclin-1/ATG6 is part of a lipid kinase complex that has been shown to play a central role in coordinating the cytoprotective function of autophagy and in opposing apoptosis (24). In addition, the activity of the lysosomal/endosomal vesicular pathway appeared to be increased in the caput epididymal epithelium of the *Ido1*$^{-/-}$ animals, as evidenced by ultrastructural features characteristic of autophagic processes, such as the intracellular accumulation of multilamellar bodies (25). Together, these data support the idea that autophagy is up-regulated in *Ido1*$^{-/-}$ caput epididymis to compensate for a decline in intracellular proteasome-dependent protein catabolism. It is interesting to note that beclin-1-mediated autophagy has been reported elsewhere to be part of an immune defense mechanism (24, 42). Thus, the hallmarks of autophagy seen in caput segment 2 of the *Ido*$^{-/-}$ animals might be associated with changes in the inflammatory situation. Determination of whether up-regulation of autophagy in the *Ido1*$^{-/-}$ caput epididymis serves an immunological role or is simply an intracellular adjustment to proteasome inhibition and defective intracellular protein catabolism will have to await further investigation. Only caput segment S2 presented microscopically detectable autophagic features suggesting that this particular segment is somehow more sensitive or involved in a specialized function. As proposed earlier, caput epididymis segment 2 may constitute a separate functional entity with immunoregulatory properties (43).

The IDO Pathway and Sperm Quality Control—Intriguingly, the caudae epididymides of IDO-deficient males yielded sperm counts that were twice those of WT mice. Because testis weights were not different between *Ido1*$^{-/-}$ and WT animals, increased spermatogenesis might not be responsible for the greater number of spermatozoa found in *Ido1*$^{-/-}$ males. In addition, fertile *Ido1*$^{-/-}$ did not show any impairment of their mating behavior, ruling out the idea that these elevated sperm counts were due to a low frequency of ejaculation. Alternatively, significantly less sperm may be lost during epididymal transit in *Ido1*$^{-/-}$ males because of an impaired sperm quality control mechanism that normally eliminates defective spermatozoa.

There is a growing body of evidence supporting the active selection, removal, and degradation of mammalian spermatozoa during epididymal transport (reviewed in Refs. 44 and 45). There are three non-exclusive major processes that have been proposed to explain how spermatozoa might be disposed of during epididymal transit (46). Two of these hypotheses involve spermiophagy by infiltrating leukocytes and/or by epithelial cells lining the epididymal duct. The third hypothesis implicates enzyme-based degradation of spermatozoa in the epididymal lumen. In support of the latter, evidence has been generated indicating that the intraluminal degradation of defective spermatozoa could occur by means of proteasomal proteolysis and extracellular nuclease activity in the epididymal lumen (47, 48). Our work brings arguments in favor of the participation of the proteasome apparatus in epididymal spermatozoa quality control processes. Our observation that increased sperm counts in the cauda epididymis of *Ido1*$^{-/-}$ animals are significantly correlated with a reduction in leukocyte count and decreased proteasome activity suggests an active mechanism for the removal of damaged, abnormal, and/or necrotic spermatozoa during their epididymal descent. Our data also indicate that proteasome-mediated degradation of spermatozoa is a process that starts as early as in the caput region, in line with evidence for the apocrine secretion of ubiquitin in this region of the epididymis (47). IDO and its downstream metabolites can be thus viewed as potent regulators of both cell-based spermiophagy and proteasome-mediated destruction of spermatozoa, two processes that appear to be heavily involved in an active sperm quality control mechanism operating in the epididymis. These observations are supported by the fact that *Ido1*$^{-/-}$ animals possess significantly greater numbers of morphologically defective spermatozoa as compared with WT controls. We propose that IDO activity on the one hand controls the level of epididymal leukocytes and, on the other hand, regulates the involvement of the epididymal proteasome in clearing defective transiting spermatozoa. Exactly how this is achieved will be the focus of future studies.

Thus, IDO expression appears essential in maintaining immunological tolerance toward spermatozoa on the one hand

while mediating an active sperm quality control system on the other. Clinically, these findings have important implications ranging from the understanding of inflammation and infectious situations in the epididymis (a significant part of male infertility cases) to the development of autoimmunity against sperm antigens as well as the poor sperm morphology that is such a consistent feature of human infertility.

Acknowledgments—We thank Agnès Claustre for excellent technical assistance in addressing the regulation of the unfolded protein stress pathway. We are indebted to Dr. Felicity Vear (Institut National de Le Recherche Agronomique) for English grammar and syntax corrections.

REFERENCES

1. Mellor, A. L., and Munn, D. H. (2004) *Nat. Rev. Immunol.* **4,** 762–774
2. Mellor, A. L., and Munn, D. H. (2008) *Nat. Rev. Immunol.* **8,** 74–80
3. Munn, D. H., and Mellor, A. L. (2007) *J. Clin. Invest.* **117,** 1147–1154
4. Beutelspacher, S. C., Tan, P. H., McClure, M. O., Larkin, D. F., Lechler, R. I., and George, A. J. (2006) *Am. J. Transplant.* **6,** 1320–1330
5. Wang, Y., Liu, H., McKenzie, G., Witting, P. K., Stasch, J. P., Hahn, M., Changsirivathanathamrong, D., Wu, B. J., Ball, H. J., Thomas, S. R., Kapoor, V., Celermajer, D. S., Mellor, A. L., Keaney, J. F., Jr., Hunt, N. H., and Stocker, R. (2010) *Nat. Med.* **16,** 279–285
6. Jalili, R. B., Forouzandeh, F., Bahar, M. A., and Ghahary, A. (2007) *Iran J. Allergy Asthma Immunol.* **6,** 167–179
7. King, N. J., and Thomas, S. R. (2007) *Int. J. Biochem. Cell Biol.* **3,** 2167–2172
8. Xu, H., Zhang, G. X., Ciric, B., and Rostami, A. (2008) *Immunol. Lett.* **121,** 1–6
9. Yoshida, R., Nukiwa, T., Watanabe, Y., Fujiwara, M., Hirata, F., and Hayaishi, O. (1980) *Arch. Biochem. Biophys.* **203,** 343–351
10. Takikawa, O., Tagawa, Y., Iwakura, Y., Yoshida, R., and Truscott, R. J. (1999) *Adv. Exp. Med. Biol.* **467,** 553–557
11. Britan, A., Maffre, V., Tone, S., and Drevet, J. R. (2006) *Cell Tissue Res.* **324,** 301–310
12. Dufaure, J. P., Lareyre, J. J., Schwaab, V., Mattei, M. G., and Drevet, J. R. (1996) *C. R. Acad. Sci. III* **319,** 559–568
13. Vazeille, E., Codran, A., Claustre, A., Averous, J., Listrat, A., Béchet, D., Taillandier, D., Dardevet, D., Attaix, D., and Combaret, L. (2008) *Am. J. Physiol. Endocrinol. Metab.* **295,** E1181–E1190
14. Combaret, L., Dardevet, D., Rieu, I., Pouch, M. N., Béchet, D., Taillandier, D., Grizard, J., and Attaix, D. (2005) *J. Physiol.* **569,** 489–499
15. Lowry, O. H., Rosebrough, N. J., Farr, A. L., and Randall, R. J. (1951) *J. Biol. Chem.* **193,** 265–275
16. Lefrançois, A. M., Jimenez, C., and Dùfaure, J. P. (1993) *Int. J. Androl.* **16,** 147–154
17. Rajapurohitam, V., Bedard, N., and Wing, S. S. (2002) *Am. J. Physiol. Endocrinol. Metab.* **282,** E739–E745
18. Metz, R., Duhadaway, J. B., Kamasani, U., Laury-Kleintop, L., Muller, A. J., and Prendergast, G. C. (2007) *Cancer Res.* **67,** 7082–7087
19. Ball, H. J., Yuasa, H. J., Austin, C. J., Weiser, S., and Hunt, N. H. (2009) *Int. J. Biochem. Cell Biol.* **41,** 467–471
20. Jenny, M., Santer, E., Pirich, E., Schennach, H., and Fuchs, D. (2009) *J. Neuroimmunol.* **207,** 75–82
21. Kimball, S. R. (2001) *Prog. Mol. Subcell. Biol.* **26,** 155–184
22. Avruch, J., Belham, C., Weng, Q., Hara, K., and Yonezawa, K. (2001) *Prog. Mol. Subcell. Biol.* **26,** 115–154
23. Nobukuni, T., Joaquin, M., Roccio, M., Dann, S. G., Kim, S. Y., Gulati, P., Byfield, M. P., Backer, J. M., Natt, F., Bos, J. L., Zwartkruis, F. J., and Thomas, G. (2005) *Proc. Natl. Acad. Sci. U.S.A.* **102,** 14238–14243
24. Cao, Y., and Klionsky, D. J. (2007) *Cell Res.* **17,** 839–849
25. Hariri, M., Millane, G., Guimond, M. P., Guay, G., Dennis, J. W., and Nabi, I. R. (2000) *Mol. Biol. Cell* **11,** 255–268
26. Baban, B., Chandler, P., McCool, D., Marshall, B., Munn, D. H., and Mellor, A. L. (2004) *J. Reprod. Immunol.* **61,** 67–77
27. Ball, H. J., Sanchez-Perez, A., Weiser, S., Austin, C. J., Astelbauer, F., Miu, J., McQuillan, J. A., Stocker, R., Jermiin, L. S., and Hunt, N. H. (2007) *Gene* **396,** 203–213
28. Liu, X. Q., and Wang, X. (2009) *Chin. Med. J.* **122,** 3072–3077
29. Zhu, B. T. (2010) *Int. J. Mol. Med.* **25,** 831–835
30. Terness, P., Bauer, T. M., Röse, L., Dufter, C., Watzlik, A., Simon, H., and Opelz, G. (2002) *J. Exp. Med.* **196,** 447–457
31. Hwu, P., Du, M. X., Lapointe, R., Do, M., Taylor, M. W., and Young, H. A. (2000) *J. Immunol.* **164,** 3596–3599
32. Wang, J., Simonavicius, N., Wu, X., Swaminath, G., Reagan, J., Tian, H., and Ling, L. (2006) *J. Biol. Chem.* **281,** 22021–22028
33. Itoh, M., Terayama, H., Naito, M., Ogawa, Y., and Tainosho, S. (2005) *) J. Reprod. Immunol.* **67,** 57–67
34. Saito, S., Nakashima, A., Shima, T., and Ito, M. (2010) *Am. J. Reprod. Immunol.* **63,** 601–610
35. Favre, D., Mold, J., Hunt, P. W., Kanwar, B., Loke, P., Seu, L., Barbour, J. D., Lowe, M. M., Jayawardene, A., Aweeka, F., Huang, Y., Douek, D. C., Brenchley, J. M., Martin, J. N., Hetch, F. M., Deeks, S. G., and McCune, J. M. (2010) *Transl. Med.* **32,** 32–36
36. Belladonna, M. L., Orabona, C., Grohmann, U., and Puccetti, P. (2009) *Trends Mol. Med.* **15,** 41–49
37. Hamel, F. G., Upward, J. L., Siford, G. L., and Duckworth, W. C. (2003) *Metabolism* **52,** 810–814
38. Bence, N. F., Sampat, R. M., and Kopito, R. R. (2001) *Science* **292,** 1552–1555
39. Levine, S. J., Adamik, B., Hawari, F. I., Islam, A., Yu, Z. X., Liao, D. W., Zhang, J., Cui, X., and Rouhani, F. N. (2005) *Am. J. Physiol. Lung Cell Mol. Physiol.* **289,** L233–L243
40. Fissolo, N., Kraus, M., Reich, M., Ayturan, M., Overkleeft, H., Driessen, C., and Weissert, R. (2008) *Eur. J. Immunol.* **38,** 2401–2411
41. Korolchuk, V. I., Menzies, F. M., and Rubinsztein, D. C. (2010) *FEBS Lett.* **584,** 1393–1398
42. Deretic, V. (2006) *Curr. Opin. Immunol.* **18,** 375–382
43. Johnston, D. S., Jelinsky, S. A., Bang, H. J., DiCandeloro, P., Wilson, E., Kopf, G. S., and Turner, T. T. (2005) *Biol. Reprod.* **73,** 404–413
44. Axnér, E. (2006) *Theriogenology* **66,** 14–24
45. Sutovsky, P. (2003) *Microsc. Res. Tech.* **61,** 88–102
46. Jones, R. (2004) *Biol. Reprod.* **71,** 1405–1411
47. Baska, K. M., Manandhar, G., Feng, D., Agca, Y., Tengowski, M. W., Sutovsky, M., Yi, Y. J., and Sutovsky, P. (2008) *J. Cell. Physiol.* **215,** 684–696
48. Dominguez, K., and Ward, W. S. (2009) *Syst. Biol. Reprod. Med.* **55,** 193–199

Deficient Tryptophan Catabolism along the Kynurenine Pathway Reveals That the Epididymis Is in a Unique Tolerogenic State

Aicha Jrad-Lamine, Joelle Henry-Berger, Pascal Gourbeyre, Christelle Damon-Soubeyrand, Alain Lenoir, Lydie Combaret, Fabrice Saez, Ayhan Kocer, Shigenobu Tone, Dietmar Fuchs, Wentao Zhu, Peter J. Oefner, David H. Munn, Andrew L. Mellor, Najoua Gharbi, Rémi Cadet, R. John Aitken and Joël R. Drevet

J. Biol. Chem. 2011, 286:8030-8042.
doi: 10.1074/jbc.M110.172114 originally published online December 28, 2010
